catalysts

MDPI

Article

Preparation of PdCu Alloy Nanocatalysts for Nitrate Hydrogenation and Carbon Monoxide Oxidation

Fan Cai [1], Lefu Yang [1,*], Shiyao Shan [2], Derrick Mott [3], Bing H. Chen [1], Jin Luo [2] and Chuan-Jian Zhong [2,*]

[1] College of Chemistry and Chemical Engineering, Xiamen University, Xiamen 361005, China; mike136136@sina.com (F.C.); chenbh@xmu.edu.cn (B.H.C.)

[2] Department of Chemistry, State University of New York at Binghamton, Binghamton, NY 13902, USA; sshan2@binghamton.edu (S.S.); jluo@binghamton.edu (J.L.)

[3] School of Materials Science, Japan Advanced Institute of Science and Technology, 1-1 Asahidai, Nomi, Ishikawa 923-1292, Japan; derrickmott@gmail.com

* Correspondence: lfyang@xmu.edu.cn (L.Y.); cjzhong@binghamton.edu (C.J.-Z.); Tel.: +86-592-139-5921-4440 (L.Y.); +86-607-777-4605 (C.J.-Z.)

Academic Editor: John R. (JR) Regalbuto

Received: 4 April 2016; Accepted: 24 June 2016; Published: 30 June 2016

Abstract: Alloying Pd with Cu is important for catalytic reactions such as denitrification reaction and CO oxidation reaction, but understanding of the catalyst preparation and its correlation with the catalyst's activity and selectivity remains elusive. Herein, we report the results of investigations of the preparation of PdCu alloy nanocatalysts using different methods and the catalytic properties of the catalysts in catalytic denitrification reaction and CO oxidation reaction. PdCu alloy nanocatalysts were prepared by conventional dry impregnation method and ligand-capping based wet chemical synthesis method, and subsequent thermochemical activation as well. The alloying characteristics depend on the bimetallic composition. PdCu/Al_2O_3 with a Pd/Cu ratio of 50:50 was shown to exhibit an optimized hydrogenation activity for the catalytic denitrification reaction. The catalytic activity of the PdCu catalysts was shown to be highly dependent on the support, as evidenced by the observation of an enhanced catalytic activity for CO oxidation reaction using TiO_2 and CeO_2 supports with high oxygen storage capacity. Implications of the results to the refinement of the preparation of the alloy nanocatalysts are also discussed.

Keywords: palladium-copper alloy; nanocatalyst; nitrate hydrogenation; CO oxidation; bimetallic composition; support effect

1. Introduction

Alloying noble metals with different transition metals have become one important focal point of research and development in the preparation of catalysts. For alloying at the nanoscale, one of the key challenges is the ability to control the alloyed nanoparticles in terms of size, shape, composition, phase structure, and the prevention of the propensity of nanoscale aggregation and sintering [1]. In recent years, palladium (Pd) alloyed with transition metals (e.g., copper (Cu), and nickel (Ni)), as an alternative to Pt based alloy catalysts, has received extensive attentions, as evidenced by the surge of studies of the preparation of low-cost, active and stable catalysts [2–22]. One intriguing system of Pd-based nanoalloy catalysts is Pd alloyed with Cu. Interests in this system continue to rise in view of the discovery of catalytic synergy of the PdCu alloy catalysts in various catalytic reactions under both gas phase and electrochemical conditions, and results from theoretical studies of this system [23,24]. For example, for Cu-rich Pd-Cu nanoalloy, CO adsorption energy was found to shift to a higher energy level significantly due to the downshift of Pd *d-band* center [25]. The arrangement of

Cu species with respect to Pd species was found to produce to an atomic ensemble effect, influencing strongly the catalytic activity [26]. These theoretical studies have been further shown to be consistent with the catalytic synergy for CO oxidation over PdCu nanoalloy catalysts of different bimetallic composition, revealing a maximum catalytic activity at a Pd:Cu ratio of 50:50. This type of catalytic synergy was also found to be dependent on the atomic scale structure, which can be tuned by the nanoparticle preparation method and thermochemical processing condition [23]. Another example involves electrocatalytic oxygen reduction reaction (ORR) over PdCu nanoalloys in acidic electrolyte, revealing a similar catalytic synergy in terms of atomic composition [24]. The result is consistent with results from DFT calculations, in which a charge transfer from Pd to Cu is revealed as a result of the reduction of Pd-O binding energy by Cu and the increase of Cu-O binding energy by Pd [27].

In addition to the interests in CO oxidation and electrocatalytic reduction of O_2 over Pd based alloy catalysts, there has also been increasing interest in studies of such catalysts in catalytic oxidation, hydrogenation, and combustion of different hydrocarbons [5–22,28–33] and in catalytic reduction of inorganic ions in solutions. One example of recent interests the catalytic reduction of nitrate pollutants in groundwater from industrial and domestic effluents. Such pollutants have become a worldwide environmental problem due to the excessive use of fertilizers in the developing countries. Several cleaning techniques have been explored for removing nitrates from water. The chemical reduction process could transform nitrate into the innocent form such as nitrogen. It would make a permanent cure for the nitrate pollution other than enrichment by reverse osmosis and electrodialysis. When using hydrogen as reducing agent, an effective catalyst is necessary for promoting the hydrogenation of NO_3^- into nitrogen and water. Some bimetallic and trimetallic catalysts such as Pd-Cu, Pd-Sn and Pd-Cu-Pt catalysts loaded on various supports have been suggested as catalysts for this denitrification reaction [34–36]. However, the formation of undesirable byproducts such as nitrite and ammonia is a main drawback in the previous studies [37]. Several experimental studies of PdCu alloys have demonstrated the importance of tuning the atomic structure and morphology of the nanoalloys for achieving better catalytic properties. In a study on CO and NO elimination over PdCu nanoalloy catalysts, the catalytic properties were found to be tunable by taking advantage of metal-active support interface interactions [38]. Another early study on CO oxidation over PdCu single crystal alloys with Pd-rich surface demonstrated an increase of surface Cu:Pd ratio from 0.1 to 0.7 due to diffusion of Cu from the bulk to the surface of Pd-Cu crystal [39]. PdCu nanoalloys on active Al_2O_3 and TiO_2 supports have been shown to exhibit high activity for CO removal in ambient atmosphere [40]. $Cu_2Cl(OH)_3$ species have also been found to improve the catalytic activity of Pd-Cu nanoalloys by promoting re-oxidation of Pd(0) to Pd(2+) species. However, little is known for the controlled preparation of the bimetallic nanocatalysts, which is important for subsequent studies of the catalytic synergy in terms of bimetallic composition and supports. There is clear need to design and prepare active and selective catalysts.

Despite of increasing studies of PdCu alloy catalysts in various catalytic reactions, understanding of the catalyst preparation and the correlation with the catalyst's activity and selectivity remains elusive. Herein, we describe the results of recent investigations of the preparation of PdCu nanoalloy catalysts using different methods and the catalytic properties of the catalysts in catalytic denitrification reaction and CO oxidation reaction. Examples will focus on PdCu alloy catalysts prepared by both conventional dry impregnation method and ligand-capping based wet chemical synthesis method, and subsequent thermochemical activation of the catalysts. Scheme 1 illustrates the basic processes of the two methods in terms of catalysts preparation, alloying properties and catalytic activities.

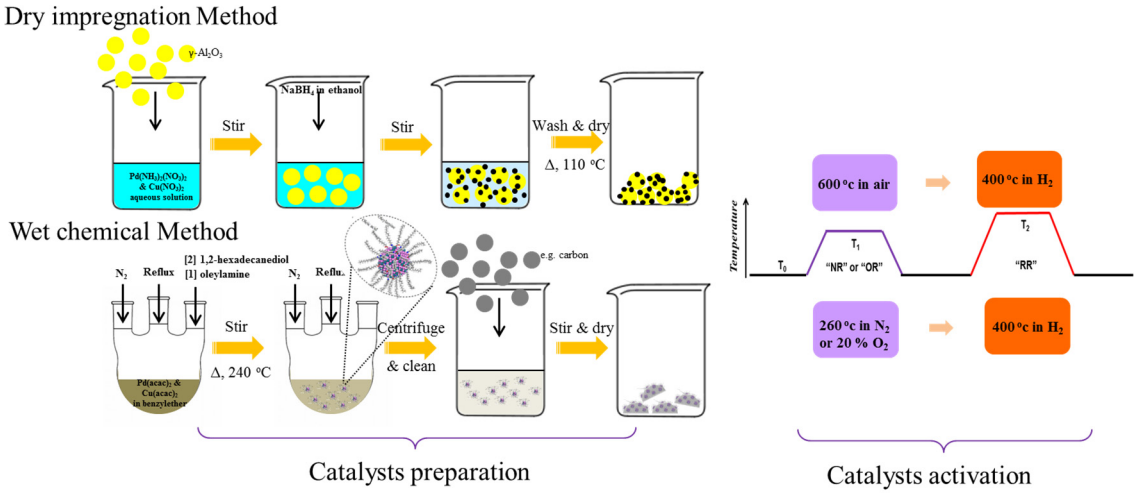

Scheme 1. Illustration of the basic processes in the two methods for the preparation of PdCu alloy nanocatalysts (**left**): dry impregnation method (**top**); and wet chemical method (**bottom**); and subsequent thermochemical activation of the nanoacatalysts (**right**).

2. Results and Discussion

2.1. Catalyst Characterizations

PdCu catalysts developed by impregnation method were firstly evaluated by nitrogen adsorption tests. It is found that the calcination treatment and the metal loading do not have significant influence on the specific surface area (SSA). The SSA was observed to be above 210 $m^2 \cdot g^{-1}$ for all catalysts. No obvious sintering or blocking by metal particles on the alumina support was observed. The elemental composition was analyzed by SEM-EDX technique (Figure S1). It is shown that the bimetallic composition basically follows the metal ratio of feedstock by dry impregnation method. Note, however, that the resolution of SEM is not high enough to assess the details of alloy particles and supports. The transmission electron microscopy (TEM) image shows that the alloy forms spherical particles with an average size of 7.7 ± 2.0 nm on alumina support in Figure 1A. The relatively broad size distribution in Figure 1B suggests that a fusing process may take place when the particles undergo thermal treatment. However, the metal dispersion does not change significantly with the composition of alloy. The dispersion of metal for the 1 wt % and 5 wt % series is about 9% and 4%, respectively, for any of the bimetallic composition. Based on this result, the difference in mass transition among the samples in the same series is considered to be insignificant.

After the calcination in air, the metal components are likely in oxidized states. Figure 2 shows a representative set of hydrogen temperature-programmed reduction (H_2-TPR) curves for the 1 wt % sample series. The Cu catalyst by impregnation method shows the classic feature of CuO reduction. With the introduction of palladium into Copper, the CuO reduction is promoted by the hydrogen spillover that is facilitated by palladium. At the same time, a reversed peak is observed at 70 °C, which is attributed to the decomposition of PdH_x. This observation indicates that the palladium still exist in element state. When the Pd/Cu ratio is increased to 50:50, the desorption of hydrogen at 70 °C disappears. The alloying between palladium and copper prohibits the behavior of one-component metal. When the Pd/Cu ratio is increased to 90:10, the reversed TPR peak reappears. These observations are illustrated in Figure 2B for alloying of the two metal components. The calcination at 600 °C fuses the two components together in partially oxidized states. When they are reduced at 50 °C in the run-up period of TPR, the catalyst with palladium content shows element metal state from partially oxidized metals. When the palladium composition is not enough to form PdCu alloy, the reduced palladium particles, which are isolated by copper component, would react with hydrogen and produce partially hydrogenated PdH_x species. PdH_x decomposes at 70 °C and

returns to metallic Pd particles, which would assist dissociation of hydrogen molecules. As a result, the reduction of CuO_x will be facilitated. Once the palladium composition is elevated to 50%, the insulation is broken and the alloying would spread across the particle. Although the resulting alloy does not lean to form hydride, it displays the consistent reducibility for both metal oxides. When the palladium composition is increased to 90%, the extra palladium forms PdH_x again and promotes the further reduction of metals in the alloy.

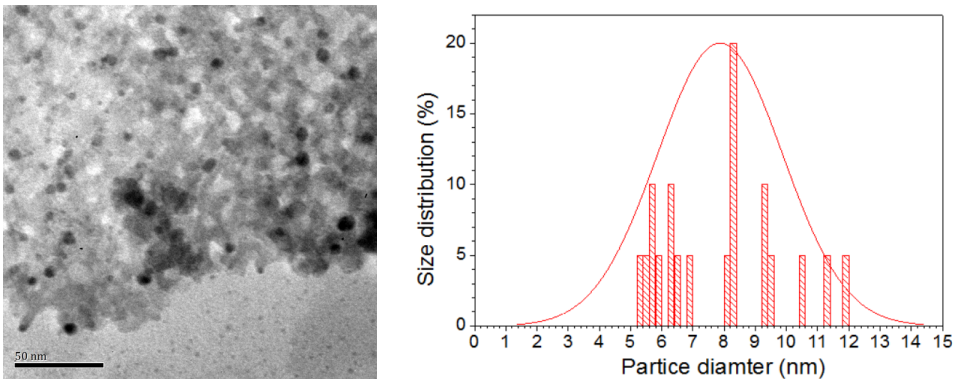

(**A**) (**B**)

Figure 1. TEM image (**A**) and size distribution (**B**) for a 5 wt % Pd-Cu (50:50) alloy particles supported on alumina, prepared by dry impregnation method.

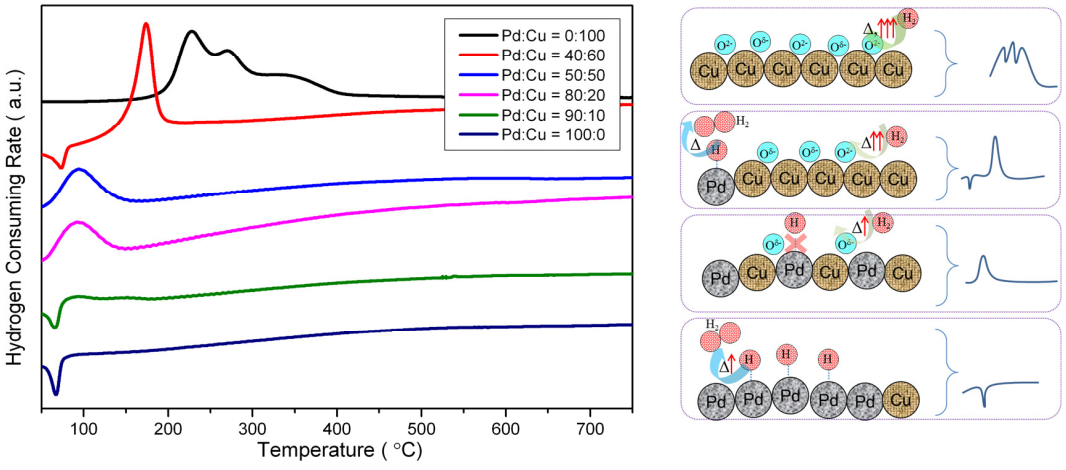

(**A**) (B)

Figure 2. (**A**) H_2-TPR patterns for catalysts of 1 wt % Pd-Cu/Al_2O_3 with different Pd/Cu ratios; and (**B**) illustrations of hydrogen adsorption/desorption on the PdCu surface corresponding to the peak characteristics in (**A**).

On the basis of the H_2-TPR results, there is a combination of alloying and phase segregation occurring in the PdCu nanoparticles of different compositions in the heating and reducing processes, as illustrated in Scheme 2. For $Pd_{40}Cu_{60}$ sample, when the palladium particles are blocked by copper component, the activated hydrogen is not able to effectively reduce the Cu-O-Cu in the bulk copper oxide. Given the high palladium loading, there is no isolated copper oxide particles inserted in this PdCu oxide precursor. Apparently, the Cu-O-Cu species has transformed into the Cu-O-Pd species as a result of the two reduction processes for both palladium and copper components in the alloy. Alloying between palladium and copper clearly has an effect on the reducibility of bimetallic catalysts. Moreover, the reducibility of metal component is believed to be a key factor contributing to the catalytic performance for denitrification of nitrate.

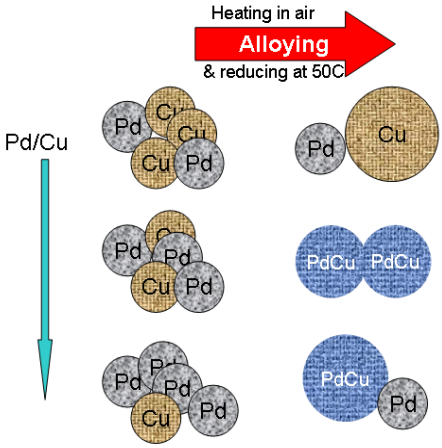

Scheme 2. Proposed the alloying and phase segregation occurring in the PdCu nanoparticles of different compositions in the heating and reducing processes.

In comparison with the alloy nanocatalysts prepared dry impregnation method, PdCu alloy nanocatalysts synthesized by wet chemical synthesis show a better control over the particle size and size monodispersity. In general, the composition of the Pd_nCu_{100-n} (n = 21, 48, and 75) alloy nanoparticles can be well controlled for each individual component as demonstrated in our previous report [23]. For example, the average sizes of Pd_nCu_{100-n} alloy nanoparticles can be controlled at 5.7 $\pm$ 0.5, 5.5 $\pm$ 0.5, and 5.5 $\pm$ 0.8 nm for n = 21, 48, and 75, respectively. For carbon supported Pd_nCu_{100-n} catalysts (n = 21, 48, and 75), after thermochemical activation, the average particle sizes are determined to be 7.4 $\pm$ 1.2, 6.0 $\pm$ 0.8, and 4.9 $\pm$ 0.5 nm, respectively, which are slightly larger than that of the corresponding as-synthesized NPs. Figure 3 shows an example for a sample of carbon supported $Pd_{21}Cu_{79}$ nanoparticles. This phenomenon is due to the slight sintering induced by the post-synthesis treatment. The particles appear spherical in shape and uniformly distributed over the carbon support with narrower size distribution than that synthesized by the dry impregnation method (Figure 3B). High angle annular dark field scanning transmission electron microscopy (HAADF-STEM) image shows that the thermochemically-treated PdCu NPs are highly crystalline (Figure 3A insert). A close examination of the lattice fringe reveals an average lattice fringe of 2.192 Å, indicative of (111) facet characteristic.

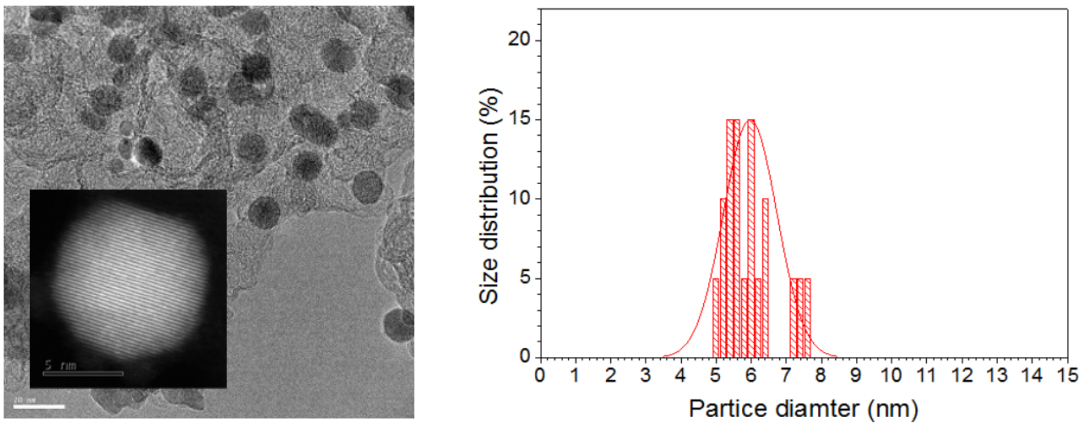

(**A**) (**B**)

Figure 3. A representative set of TEM and high-resolution TEM (HRTEM) image (**A**); and size distribution (**B**) for a sample of $Pd_{21}Cu_{79}$ nanoparticles. Note that the scale bars are 20 nm and 5 nm for the TEM and the inserted HRTEM images, respectively.

The distribution of Pd and Cu species across the treated nanoparticles, i.e., the chemical composition mapping, was further analyzed by HAADF-STEM and energy dispersive spectroscopy (EDS) mapping analysis. A representative set of results is shown in Figure 3A insert and Figure 4. It is evident that Pd and Cu species are uniformly distributed across the NPs, confirming their alloy-type character (Figure 4).

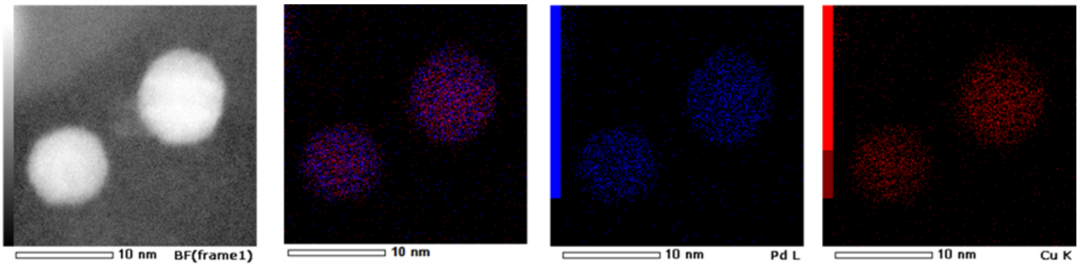

Figure 4. A representative set of EDS mapping data showing the elemental distribution across the nanoparticle for a sample of $Pd_{20}Cu_{80}$ nanoparticles.

For the impregnated PdCu catalysts, the SEM-EDX result for the alumina supported sample (see Figure S1) was complicated by the lack of resolution due to significant aggregation of the particles. While a further detailed study is needed, the results show that the wet chemical method prepared catalysts are better controlled than the impregnation prepared catalysts.

To determine the relative surface distribution and oxidation states of Pd and Cu species for the PdCu alloy catalysts, XPS analysis was carried out (Figure 5). The relative surface composition is found to be similar to the bulk chemical composition of PdCu alloy NPs, consistent with the alloy properties of PdCu catalysts prepared by the wet chemical method. The binding energy of Pd species for PdCu NPs appears to show a minimum for Pd:Cu ratio at ~50:50. For Cu species, the peak characteristic appears to change significantly with the bimetallic composition with additional peaks, implying Cu(+2/+1) species present in a Cu-rich PdCu alloy. The partial oxidation of Cu in PdCu alloy NPs with Pd/Cu ratio <50:50 is very likely due to air exposure before XPS analysis. More in-depth in-situ XPS experiments to further determine the valence state changes during the reactions are part of our future work.

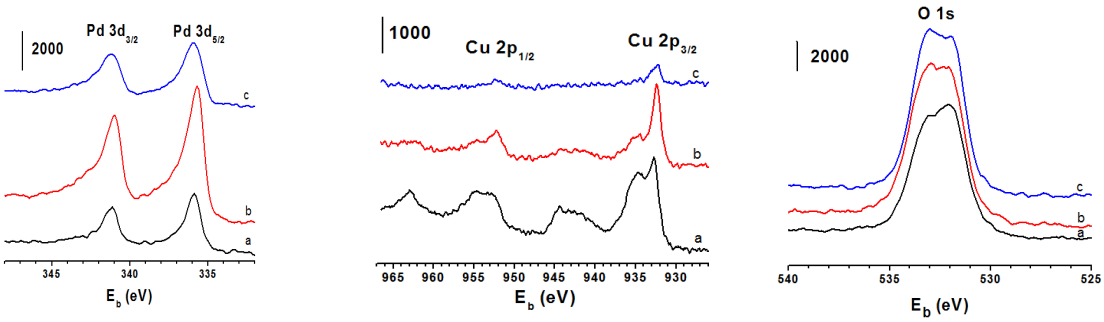

Figure 5. XPS spectra of carbon-supported $Pd_{21}Cu_{79}/C$ (black, **a**), $Pd_{48}Cu_{52}/C$ (red, **b**) and $Pd_{75}Cu_{25}/C$ (blue, **c**) in regions of: Pd 3d (**A**); Cu 2p (**B**); and O 1s (**C**).

2.2. *Catalytic Activity Evaluation*

2.2.1. Catalytic Denitrification

PdCu catalysts prepared by impregnation method were examined for catalytic denitrification reaction. Data for the catalytic activity are shown in Figure 6. Figure 6a shows the product distribution

after denitrification test over 1 wt % Pd-Cu supported on alumina. It was found that the palladium is indispensable for the reduction of nitrate, since the copper mono-component catalyst shows no hydrogenation activity. When the Pd/Cu ratio increases to 40:60, 68% of nitrate is reduced into nitrite form by hydrogen. There is an indication of further reduction. When the PdCu is in the alloy region as controlled by the Pd:Cu ratio, the deep hydrogenation is initiated. If the Pd/Cu goes beyond the alloy region, the nitrate hydrogenation catalytic activity shows a dramatic drop. However, the nitrite product, which is more harmful to human health, is eliminated. In the case of pure palladium catalyst, there is a lower denitrification activity.

If a higher metal loading is adopted, a higher hydrogenation activity is acquired, as expected. Furthermore, the same tendency in terms of alloying degree is also observed for the 5 wt % sample series. On the alloy catalysts (Pd/Cu = 50:50, and 80:20), the composition of nitrite product is muffled to 18% and 23%, respectively. A 45% selectivity of nitrogen is achieved on both samples. For low loading samples, once the Pd/Cu ratio exceeds that corresponding to the alloying region, a decrease of the hydrogenation activity is observed.

It is known that both NO_3^- adsorption and hydrogen dissociation are key steps for the denitrification reaction following Langmiur-Hinshelwood mechanism. When the palladium is the exclusive adsorption site, it is difficult for the combination of electrophilicity and electron feedback to be operative for both reactants. In the case of the low loading sample, the positive charge transferred from support prevents the effective activation of hydrogen molecules. Only upon the introduction of copper, the overlapping of *d* orbit from Pd and Cu neutralizes the hindrance of hydrogen adsorption and activation. However, when Pd/Cu ratio is lower than 50:50, the adsorption of NO_3^- becomes too weak to achieve effective adsorption on the alloy. This is because the surface of the high copper containing alloy becomes more electrophilic. An optimized Pd/Cu ratio is identified to be about 50:50 for both 1 wt % and 5 wt % loading samples, as shown in Figure 5.

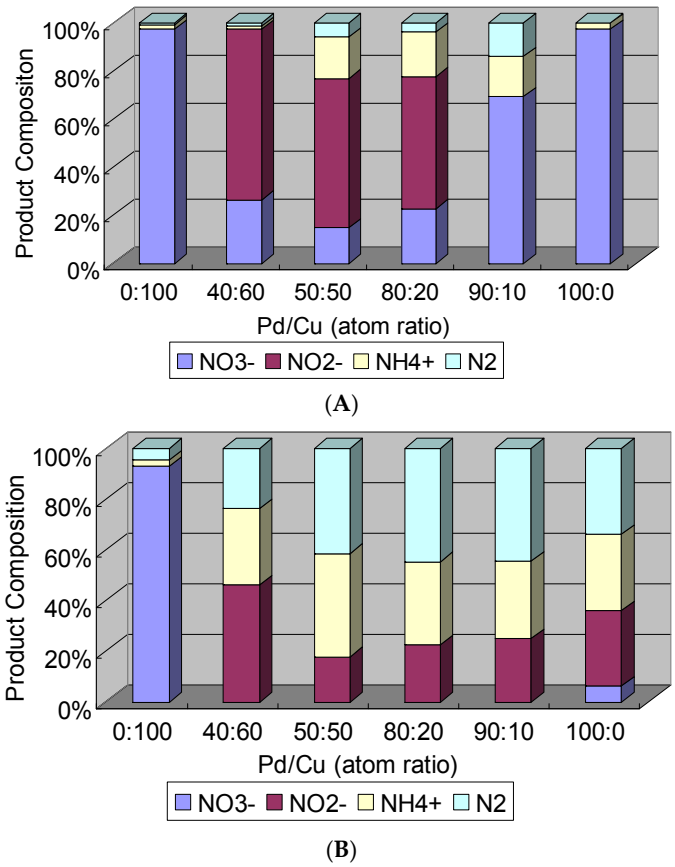

Figure 6. Product compositions of denitrification reaction catalyzed by Pd-Cu/Al_2O_3 with different Pd/Cu ratios under two different loading: (**A**) 1 wt %; and (**B**) 5 wt % metal/alloy loading samples.

We also note that the same tendency has been displayed on PdCu/ACC and PdAg/Al_2O_3 catalysts for denitrification [41,42]. In these two catalytic reactions, palladium is assigned as the active phase for hydrogen activation and the consecutive hydrogenation sites for nitrite. However, the adsorption of nitrate hardly occurs without the introduction of copper. In this study, for the higher palladium loading sample, the interaction between palladium and alumina support could induce the positive charge into the metal particles, leading to the reduction of nitrate with a less extent. The acidic sites on the surface of alumina support still have an important influence on the continuous hydrogenation of nitrate. Therefore, a rather low conversion (<10%) of nitrate is obtained in the denitrification catalyzed by $Pd_{48}Cu_{52}$ supported on carbon.

2.2.2. Catalytic CO Oxidation

CO oxidation was also studied over $Pd_{48}Cu_{52}$ alloy nanoparticles deposited on different supports, which are prepared by the wet chemical synthesis method. A representative set of CO conversion data for the PdCu alloy nanocatalysts treated under H_2 atmosphere at 300 °C for 30 min is shown in Figure 7. The results indicate that PdCu nanoparticles supported on TiO_2 shows the highest catalytic activity. The catalytic activity diminishes in the order of TiO_2 > CeO_2 > SiO_2 > C > Al_2O_3, indicating an important role played by the nanoparticle-support interaction and the oxygen storage capacity of the support in the catalytic reaction.

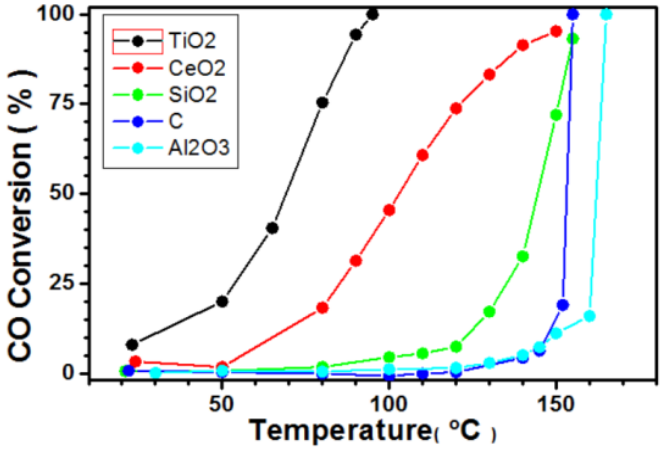

Figure 7. CO conversion for catalytic CO oxidation over $Pd_{48}Cu_{52}$ alloy NPs on different supports: TiO_2 (black), CeO_2 (green), SiO_2 (red), carbon (blue) and Al_2O_3 (cyan).

The catalytic activity for the PdCu alloy nanoparticles deposited on different supports and then subjected to an oxidative (under O_2 at 450 °C for 30 min) or reductive (under H_2 at 300 °C for 30 min) treatments are further examined. A representative set of values of T_{50} is shown in Figure 8. It is evident that the reduced nanocatalysts exhibit a higher activity than the oxidized ones.

Moreover, oxygen storage capacity is shown to play a role in enhancing the overall catalytic activity. This is evidenced by comparing the data for the different supports: "active" supports such as TiO_2 and CeO_2 show clear promotion for the oxidation of CO over PdCu alloy nanocatalysts in comparison with those "inert" supports such as SiO_2 or Al_2O_3. However, considering that the oxygen storage capacity of active supports can be severely influenced by thermochemical processing conditions for the catalysts [38,39], we believe that there are large differences for oxidized catalysts and much smaller differences for reduced catalysts on TiO_2 and CeO_2 supports. However, the $Pd_{50}Cu_{50}/Al_2O_3$ synthesized by dry impregnation method shows a good catalytic performance for CO oxidation even with an "inert" support (Figure S2). It is likely that not only the intrinsic property of support but also the supporting protocol impacts on the activity of PdCu alloys for catalytic oxidation. The modification of interaction between the alloy and support induced by synthesis would still be a good topic for

further investigation. Because of the difference between impregnation method and the wet chemical method prepared catalysts, the results on the nitrite hydrogenation reaction over the wet chemical method prepared catalysts are not included in this report for comparison. An effective comparison of the catalytic activities of these catalysts in different catalytic reactions is part of future work.

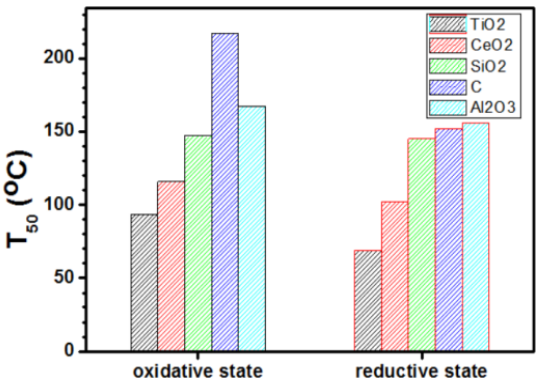

Figure 8. Comparison of T_{50} values for $Pd_{48}Cu_{52}$ catalysts over different supports (i.e., TiO_2 (black), CeO_2 (green), SiO_2 (red), carbon (blue) and Al_2O_3 (cyan)) initially treated at 260 °C under N_2 and then under reductive under 15 vol % H_2 at 400 °C followed by further treatment either under O_2 at 450 °C for 30 min, denoted on the plot as oxidized state, or under H_2 at 300 °C for 30 min, denoted on the plot as reduced state.

3. Experimental Section

3.1. Chemicals

Palladium (II) acetylacetonate ($Pd(acac)_2$, 97%), copper (II) acetylacetonate ($Cu(acac)_2$, 97%), benzyl ether ($(C_6H_5CH_2)_2O$, >98%), oleylamine ($CH_3(CH_2)_7CH$ $CH(CH_2)_8NH_2$, 70%), 1,2-hexadecanediol (90%), and oleic acid ($CH_3(CH_2)_7CH{=}CH(CH_2)_7COOH$, 99+%) were purchased from Aldrich (St Louis, MO, USA). $Pd(NH_3)_4(NO_3)_2$ and $Cu(NO_3)_2 \cdot 3H_2O$ were purchased from STREM. γ-Al_2O_3 was from Catalyst Plant of Nankai University. Other chemicals such as ethanol, hexane, copper choloride and sodium borohydrate ($NaBH_4$) were purchased from Fisher Scientific. Vulcan carbon XC-72 was from Cabot. Pd (20% on activated carbon (Pearlman's catalyst), unreduced, 50% water wet paste (Escat™ 1951, BASF Kit, New York, NY, USA)) was obtained from Strem Chemicals (Newburyport, MA, USA). Gases of CO (1 vol % balanced by N_2) and O_2 (20 vol % balanced by N_2) were purchased from Airgas (Radnor, PA, USA). All chemicals were used as received.

3.2. Catalyst Preparations

3.2.1. Dry Impregnation Method

The support γ-Al_2O_3 (specific surface area, 233 $m^2 \cdot g^{-1}$) was supplied by the Catalyst Plant of Nankai University. Before the metal loading, the alumina support was ground by mortar and sieved. The powder with the size smaller than 300 mesh per square inch was used as actual support. The metal salts with the form of $Pd(NH_3)_4(NO_3)_2$ and $Cu(NO_3)_2$ (both from STREM, Newburyport, MA, USA) were mixed in aqueous solution. With the intent of incipient wetness, the saturated solutions of corresponding metal salts were dripped into the powder in order to obtain slurry. Then the $NaBH_4$ solved in ethanol was dripped into the slurry under stirring. The resulting slurry was continuously stirred for 1 h until the solvent vaporized and the slurry turned into paste. After the paste was washed by water and dried at 110 °C for 24 h, the samples were calcined at 600 °C for 2 h. After this calcination pretreatment in air, the samples used for catalytic activity evaluation would be further reduced in hydrogen at 400 °C. In this paper, 1 wt % and 5 wt % metal (total quantity of palladium and copper) loading samples series were prepared. The Pd/Cu ratios were 0:100, 40:60, 50:50, 80:20, 90:10 and 100:0.

3.2.2. Catalyst Preparation by Wet Chemical Synthesis

PdCu alloy catalysts by wet chemical method follows a pathway from as-synthesized alloy nanoparticles to supported catalysts. Typically, PdCu alloy nanoparticles were firstly synthesized by the following protocol reported previously [22], palladium (II) acetylacetonate and copper (II) acetylacetonate in a controlled molar ratio were dissolved into Benzyl ether solvent. 1,2-hexadecanediol was added as a reducing agent. Temperature was increased slowly to 105 °C until the metal precursors started to decompose and the solution turned dark, at which point oleic acid and oleylamine were added as capping agents under N_2 atmosphere. The mixture was heated up to 220 °C with reflux for 0.5 h and then cooled down to room temperature. NPs were precipitated out by adding ethanol and centrifuging, and then dispersed in hexane solvent for further use. The active catalysts were prepared from the as-synthesized PdCu alloy NPs as follows. First, the alloy NPs were deposited on powder supports (e.g., carbon, TiO_2, SiO_2, CeO_2 and Al_2O_3) by adding a controlled amount of as-synthesized NPs to the suspension of support powder in hexane, followed by sonication and overnight stirring. The resulting carbon supported NPs were then collected by removing the solvent and dried under N_2. Second, carbon supported NPs were activated by a controlled thermochemical treatment [43,44]. In brief, the treatment involved treating of carbon supported NPs at 260 °C under O_2 or N_2 atmosphere for 1 h to remove the organic capping molecules, and further treating at 400 °C under 15% H_2–85% N_2 atmosphere for 2 h for calcination in a programmable furnace. The catalysts, termed as fresh catalysts, were loaded in a custom-built thermally-controlled reactor for further thermochemical treatment and catalytic activity testing. Commercial carbon supported Pd NPs (Pd/C) was treated at 400 °C under 15% H_2 balanced by N_2 for 1 h, yielding a loading of 20 wt % Pd NPs on carbon support. For most carbon supported PdCu nanoalloy catalysts (PdCu/C), the NP weight loading on the carbon support was close to 20% (15% for $Pd_{21}Cu_{79}$/C, 23% for $Pd_{48}Cu_{52}$/C, and 15% for $Pd_{75}Cu_{25}$/C) as determined by thermogravimetric analysis (TGA) performed on a Perkin-Elmer Pyris 1-TGA instrument. TEM analysis showed that the sizes of Pd_nCu_{100-n} alloy NPs were 5.7 ± 0.5, 5.5 ± 0.5, and 5.5 ± 0.8 nm for n = 21, 54, and 75, respectively.

3.3. Catalytic Activity Measurements

3.3.1. Denitrification Activity Measurement

The catalytic tests were performed in an autoclave reactor, equipped with a magnetic stirrer and a thermostatic jacket, at 40 °C and atmospheric pressure. One hundred milliliters of 100-ppm $NaNO_3$ solution and 100 mg of catalyst were fed into the reactor, the hydrogen (flow rate = 100 mL/min) was passed through the reactor. After purging the air out (about 15 min), the magnetic stirrer was adjusted to 500 rpm to initiate the reaction. After 2 h reaction, nitrate and nitrite ions were simultaneously determined by HPLC using a Hitachi Elite Lachrom apparatus (Tokyo, Japan) equipped with a UV-vis detector (Tokyo, Japan). Nitrogen was analyzed by a quadrupole mass spectrometer (Baltzers Omnistar QMS 200 O). The yield of ammonia was calculated by subtraction of the composition of nitrate, nitrite and nitrogen.

3.3.2. CO Oxidation Activity Measurement

The catalytic activity of PdCu nanoalloy catalysts for catalytic CO oxidation reaction carried out under (0.5 vol % CO + 10 vol % O_2 balanced by N_2) atmosphere was measured using a customer-built system including a temperature-controlled reactor, gas flow/mixing/injection controllers, and an on-line gas chromatograph (Shimadzu GC 8A, Overland Park, KS, USA) equipped with 5A molecular sieve, Porapak Q packed columns and a thermal conductivity detector. The activated nanoalloys were loaded in the middle of a quartz micro-reactor tube (inner diameter: 4 mm) and wrapped by quartz wool forming a "catalyst bed" with a length of 6 mm. The feeding gas (0.5 vol % CO + 10 vol % O_2 balanced by N_2) was injected continuously through the fixed catalyst bed in the quartz micro-reactor at a flow rate of 20 mL/min. The residence time was about 0.2 s. Gas hourly space velocity (GHSV) in

the system was around 16,000 h^{-1}. Temperature control was achieved by a furnace coupled with a temperature controller. The catalytic activity for CO oxidation was determined by analyzing the tail gas effusing from the quartz micro reactor using on-line gas chromatograph.

3.4. Instrumentation Used for Characterizations of Catalysts

High-angle annular dark-field scanning TEM (HAADF-STEM, JAIST, Ishikawa, Japan) was used to characterize the morphology of Pd-Cu alloy NPs. Energy dispersive X-ray spectroscopy (EDS) was used to obtain elemental mapping and determine the chemical species pattern of PdCu alloy NPs. Experiments were carried out on an a JEOL JEM 2010F (Tokyo, Japan) with an acceleration voltage of 200 kV and a routine point-to-point resolution of 0.194 nm. TEM analysis was performed on an FEI Tecnai T12 Spirit Twin TEM/SEM electron microscope (120 kV) (Tokyo, Japan). The nanoparticle samples were suspended in hexane solution and were drop cast onto a carbon-coated copper grid followed by solvent evaporation in air at room temperature.

Inductively Coupled Plasma-Optical Emission Spectroscopy (ICP-OES) (Waltham, MA, USA) was used to determine the overall chemical composition of PdCu NPs. Measurements were performed on a Perkin Elmer 2000 DV ICP-OES instrument utilizing a Meinhardt nebulizer coupled to a cyclonic spray chamber to increase analyte sensitivity with the following parameters: 18.0 L $Ar_{(g)}$/min; auxiliary 0.3 L $Ar_{(g)}$/min; nebulizer 0.63 L $Ar_{(g)}$/min; power 1500 W; peristaltic pump rate 1.00 mL/min. Laboratory check standards were analyzed for every 6 or 12 samples and the instrument was re-calibrated if the check standards were not within $\pm$5% of the initial concentration.

X-ray photoelectron spectroscopy (XPS) measurements were performed ex-situ using a Physical Electronics Quantum 2000 scanning ESCA microprobe (Eden Prairie, MN, USA). This instrument was equipped with a focused monochromatic Al Kα X-ray (1486.7 eV) source for excitation, a spherical section analyzer and a 16-element multichannel detection system. The X-ray beam was approximately 100-μm in diameter. It was rastered over a 1.4 mm by 0.2 mm rectangle spot on the sample. During rastering the incident X-ray beam was normal to the sample while the X-ray detector tilted at 45° away from the normal. The binding energy (BE) of chemical species adsorbed at the NP surface was calibrated using C 1s peak at 284.8 eV as an internal standard. The percentages of individual elements detected were determined by analyzing the areas of the respective peaks.

4. Conclusions

In summary, PdCu alloy nanocatalysts are prepared using conventional dry impregnation method and ligand-capping based wet chemical synthesis method followed by thermochemical activation. While the dry impregnation method is highly scalable, the wet chemical reduction synthesis shows a better control over the particle size and size monodispersity. The alloying characteristics depend on the bimetallic composition, and a catalytic synergy is revealed, with $PdCu/Al_2O_3$ with a Pd/Cu ratio of 50:50 exhibiting an optimized hydrogenation activity for the catalytic denitrification reaction. Although palladium is necessary for catalytic denitrification, the redundant palladium component would inhibit the catalytic activity. The catalytic activity of the PdCu catalysts was shown to be highly dependent on the support, as evidenced by the observation of an enhanced catalytic activity for CO oxidation reaction for TiO_2 and CeO_2 supports with high oxygen storage capacity. Understanding these findings is important for refinement of the preparation of PdCu alloy nanocatalysts with better control over the size and composition.

Supplementary Materials: The following are available online at www.mdpi.com/2073-4344 /6/7/96/s1, Figure S1: SEM image (A) and EDX result (B) for a 5 wt % Pd-Cu (50:50) alloy particles supported on alumina, prepared by dry impregnation method, Figure S2: CO conversion for catalytic CO oxidation over 5 wt % Pd-Cu (50:50) alloy particles supported on alumina, prepared by dry impregnation method.

Acknowledgments: This work was supported by DOE-BES grant (DE-SC0006877) and in part by NSFC grant (21373171). We also thank Mark Engelhard from EMSL, Pacific Northwest National Laboratory, for assistance in XPS analysis.

Author Contributions: Cai, F. and Shan, S. conceived and designed the experiments; Cai, F., Yang, L., Shan S. and Mott, D. performed the experiments; Yang, L, Chen, B.H., Luo, J. and Zhong, C.J. analyzed the data; all of the authors wrote the paper.

Conflicts of Interest: The authors declare no conflict of interest.

References

1. Zhong, C.J.; Regalbuto, J.R. Metal Nanoparticle Synthesis. Surface Inorganic Chemistry and Heterogeneous Catalysis. In *Comprehensive Inorganic Chemistry II*; Schloegl, R., Niemantsverdriet, J.W., Reedijk, J., Poeppelmeier, K., Eds.; Elsevier: Amsterdam, The Netherlands, 2013; Chapter 4; Volume 7.
2. Zhang, H.; Jin, M.S.; Xia, Y.N. Enhancing the catalytic and electrocatalytic properties of Pt-based catalysts by forming bimetallic nanocrystals with Pd. *Chem. Soc. Rev.* **2012**, *41*, 8035–8049. [CrossRef] [PubMed]
3. Zhang, H.J.; Watanabe, T.; Okumura, M.; Haruta, M.; Toshima, N. Catalytically highly active top gold atom on palladium nanocluster. *Nat. Mater.* **2012**, *11*, 49–52.
4. Hutchings, G.J. Nanocrystalline gold and gold-palladium alloy oxidation catalysts: A personal reflection on the nature of the active sites. *Dalton Trans.* **2008**, 5523–5536. [CrossRef] [PubMed]
5. Chen, M.S.; Kumar, D.; Yi, C.W.; Goodman, D.W. The promotional effect of gold in catalysis by palladium-gold. *Science* **2005**, *310*, 291–293. [CrossRef] [PubMed]
6. Gao, F.; Goodman, D.W. Pd-Au bimetallic catalysts: Understanding alloy effects from planar models and (supported) nanoparticles. *Chem. Soc. Rev.* **2012**, *41*, 8009–8020. [CrossRef] [PubMed]
7. Hutchings, G.J.; Kiely, C.J. Strategies for the Synthesis of Supported Gold Palladium Nanoparticles with Controlled Morphology and Composition. *Acc. Chem. Res.* **2013**, *46*, 1759–1772. [CrossRef] [PubMed]
8. Shao, M.H.; Sasaki, K.; Adzic, R.R. Pd-Fe nanoparticles as electrocatalysts for oxygen reduction. *J. Am. Chem. Soc.* **2006**, *128*, 3526–3527. [CrossRef] [PubMed]
9. Shao, M.H.; Shoemaker, K.; Peles, A.; Kaneko, K.; Protsailo, L. Pt Mono layer on Porous Pd-Cu Alloys as Oxygen Reduction Electrocatalysts. *J. Am. Chem. Soc.* **2010**, *132*, 9253–9255. [CrossRef] [PubMed]
10. Enache, D.I.; Edwards, J.K.; Landon, P.; Solsona-Espriu, B.; Carley, A.F.; Herzing, A.A.; Watanabe, M.; Kiely, C.J.; Knight, D.W.; Hutchings, G.J. Solvent-free oxidation of primary alcohols to aldehydes using Au-Pd/TiO_2 catalysts. *Science* **2006**, *311*, 362–365. [CrossRef] [PubMed]
11. Kesavan, L.; Tiruvalam, R.; Ab Rahim, M.H.; Saiman, M.I.; Enache, D.I.; Jenkins, R.L.; Dimitratos, N.; Lopez-Sanchez, J.A.; Taylor, S.H.; Knight, D.W.; et al. Solvent-Free Oxidation of Primary Carbon-Hydrogen Bonds in Toluene Using Au-Pd Alloy Nanoparticles. *Science* **2011**, *331*, 195–199. [CrossRef] [PubMed]
12. Antolini, E. Catalysts for direct ethanol fuel cells. *J. Power Sources* **2007**, *170*, 1–12. [CrossRef]
13. Cargnello, M.; Delgado Jaen, J.J.; Hernandez Garrido, J.C.; Bakhmutsky, K.; Montini, T.; Calvino Gamez, J.J.; Gorte, R.J.; Fornasiero, P. Exceptional Activity for Methane Combustion over Modular Pd@CeO_2 Subunits on Functionalized Al_2O_3. *Science* **2012**, *337*, 713–717. [CrossRef] [PubMed]
14. Paalanen, P.; Weckhuysen, B.M.; Sankar, M. Progress in controlling the size, composition and nanostructure of supported gold-palladium nanoparticles for catalytic applications. *Catal. Sci. Technol.* **2013**, *3*, 2869–2880. [CrossRef]
15. Ward, T.; Delannoy, L.; Hahn, R.; Kendell, S.; Pursell, C.J.; Louis, C.; Chandler, B.D. Effects of Pd on Catalysis by Au: CO Adsorption, CO Oxidation, and Cyclohexene Hydrogenation by Supported Au and Pd-Au Catalysts. *ACS Catal.* **2013**, *3*, 2644–2653. [CrossRef]
16. Greeley, J.; Stephens, I.E.; Bondarenko, A.S.; Johansson, T.P.; Hansen, H.A.; Jaramillo, T.F.; Rossmeisl, J.; Chorkendorff, I.; Norskov, J.K. Alloys of platinum and early transition metals as oxygen reduction electrocatalysts. *Nat. Chem.* **2009**, *1*, 552–556.
17. Jin, C.C.; Sun, X.J.; Chen, Z.D.; Dong, R.L. Electrocatalytic activity of PdNi/C catalysts for allyl alcohol oxidation in alkaline solution. *Mater. Chem. Phys.* **2012**, *135*, 433–437. [CrossRef]
18. Xu, C.X.; Liu, A.H.; Qiu, H.J.; Liu, Y.Q. Nanoporous PdCu alloy with enhanced electrocatalytic performance. *Electrochem. Commun.* **2011**, *13*, 766–769. [CrossRef]
19. Yin, Z.; Zhou, W.; Gao, Y.J.; Ma, D.; Kiely, C.J.; Bao, X.H. Supported Pd-Cu Bimetallic Nanoparticles That Have High Activity for the Electrochemical Oxidation of Methanol. *Chem. Eur. J.* **2012**, *18*, 4887–4893. [CrossRef] [PubMed]

20. Gobal, F.; Arab, R. A preliminary study of the electro-catalytic reduction of oxygen on Cu-Pd alloys in alkaline solution. *J. Electroanal. Chem.* **2010**, *647*, 66–73. [CrossRef]
21. Fouda-Onana, F.; Bah, S.; Savadogo, O. Palladium-copper alloys as catalysts for the oxygen reduction reaction in an acidic media I: Correlation between the ORR kinetic parameters and intrinsic physical properties of the alloys. *J. Electroanal. Chem.* **2009**, *636*, 1–2. [CrossRef]
22. Yin, J.; Shan, S.; Ng, M.S.; Yang, L.F.; Mott, D.; Fang, W.; Kang, N.; Luo, J.; Zhong, C.J. Catalytic and Electrocatalytic Oxidation of Ethanol over Palladium-Based Nanoalloy Catalysts. *Langmuir* **2013**, *29*, 9249–9258. [CrossRef] [PubMed]
23. Shan, S.; Petkov, V.; Prasai, B.; Wu, J.; Joseph, P.; Skeete, Z.; Kim, E.; Malis, D.M.O.; Luo, J.; Zhong, C.J. Catalytic Activity of Bimetallic Catalysts Highly Sensitive to Atomic Composition and Phase Structure at the Nanoscale. *Nanoscale* **2015**, *7*, 18936–18948. [CrossRef] [PubMed]
24. Wu, J.; Shan, S.; Luo, J.; Joseph, P.; Petkov, V.; Zhong, C.J. PdCu Nanoalloy Electrocatalysts in Oxygen Reduction Reaction: Role of Composition and Phase Properties in Catalytic Synergy. *ACS Appl. Mater. Interfaces* **2015**, *7*, 25906–25913. [CrossRef] [PubMed]
25. Lopez, N.; Norskov, J.K. Synergetic effects in CO adsorption on Cu-Pd(111) alloys. *Surf. Sci.* **2001**, *477*, 59–75. [CrossRef]
26. Jeroro, E.; Hyman, M.P.; Vohs, J.M. Ensemble vs. electronic effects on the reactivity of two-dimensional Pd alloys: A comparison of CO and CH_3OH adsorption on Zn/Pd(111) and Cu/Pd(111). *Phys. Chem. Chem. Phys.* **2009**, *11*, 10457–10465. [CrossRef] [PubMed]
27. Tang, W.J.; Zhang, L.; Henkelman, G. Catalytic Activity of Pd/Cu Random Alloy Nanoparticles for Oxygen Reduction. *J. Phys. Chem. Lett.* **2011**, *2*, 1328–1331. [CrossRef] [PubMed]
28. Shen, S.Y.; Zhao, T.S.; Xu, J.B.; Li, Y.S. Synthesis of PdNi catalysts for the oxidation of ethanol in alkaline direct ethanol fuel cells. *J. Power Sources* **2010**, *195*, 1001–1006. [CrossRef]
29. Persson, K.; Ersson, A.; Jansson, K.; Iverlund, N.; Jaras, S. Influence of co-metals on bimetallic palladium catalysts for methane combustion. *J. Catal.* **2005**, *231*, 139–150. [CrossRef]
30. Kanra, B.C.; Bertolini, J.C.; Rousset, J.L. Effect of surface segregation on the catalytic activity of alloys: CO hydrogenation on Pd-Ni(111) surface. *J. Mol. Catal. A Chem.* **1998**, *129*, 233–240. [CrossRef]
31. Yuan, X.; Sun, G.; Asakura, H.; Tanaka, T.; Chen, X.; Yuan, Y.; Laurenczy, G.; Kou, Y.; Dyson, P.J.; Yan, N. Development of palladium surface enriched heteronuclear Au Pd nanoparticle dehalogenation catalysts in an ionic liquid. *Chem. Eur. J* **2013**, *19*, 1227–1234. [CrossRef] [PubMed]
32. Zhang, B.; Yuan, Y.; Philippot, K.; Yan, N. Ag-Pd and CuO-Pd nanoparticles in a hydroxyl-group functionalized ionic liquid: Synthesis, characterization and catalytic performance. *Catal. Sci. Technol.* **2015**, *5*, 1683–1692. [CrossRef]
33. Niu, W.X.; Gao, Y.J.; Zhang, W.Q.; Yan, N.; Lu, X.M. Pd-Pb Alloy Nanocrystals with Tailored Composition for Semihydrogenation: Taking Advantage of Catalyst Poisoning. *Angew. Chem. Int. Ed.* **2015**, *54*, 8271–8274. [CrossRef] [PubMed]
34. Soares, O.S.G.P.; Orfao, J.J.M.; Pereira, M.F.R. Bimetallic catalysts supported on activated carbon for the nitrate reduction in water: Optimization of catalysts composition. *Appl. Catal. B Environ.* **2009**, *91*, 441–448. [CrossRef]
35. Wada, K.; Hirata, T.; Hosokawa, S.; Iwamoto, S.; Inoue, M. Effect of supports on Pd–Cu bimetallic catalysts for nitrate and nitrite reduction in water. *Catal. Today* **2012**, *185*, 81–87. [CrossRef]
36. Francha, C.; Rodríguez-Castellón, E.; Reyes-Carmona, Á.; Palomares, A.E. Characterization of (Sn and Cu)/Pd catalysts for the nitrate reduction in natural water. *Appl. Catal. A Gen.* **2012**, *425–426*, 145–152. [CrossRef]
37. Soares, O.S.G.P.; Orfao, J.J.M.; Pereira, M.F.R. Nitrate reduction with hydrogen in the presence of physical mixtures with mono and bimetallic catalysts and ions in solution. *Appl. Catal. B Environ.* **2011**, *102*, 424–432. [CrossRef]
38. Fernandez-Garcia, M.; Martinez-Arias, A.; Belver, C.; Anderson, J.A.; Conesa, J.C.; Soria, J. Behavior of palladium–copper catalysts for CO and NO elimination. *J. Catal.* **2000**, *190*, 387–395. [CrossRef]
39. Lobodacackovic, J.; Hammoudeh, A.; Mousa, M.S.; Block, J.H. Oxidation of CO on PdCu(110) single crystal alloy catalyst: Steady state, hysteresis and related surface phenomena. *Vacuum* **1995**, *46*, 411–415. [CrossRef]
40. Wang, F.G.; Zhang, H.J.; He, D.N. Catalytic oxidation of low-concentration CO at ambient temperature over supported Pd-Cu catalysts. *Environ. Technol.* **2014**, *35*, 347–354. [CrossRef] [PubMed]

41. Matatov-Meytal, U.; Sheintuch, M. The relation between surface composition of Pd-Cu/ACC catalysts prepared by selective deposition and their denitrification behavior. *Catal. Commun.* **2009**, *10*, 1137–1141. [CrossRef]
42. Witońska, I.; Karski, S.; Gołuchowska, J. Hydrogenation of nitrate in water over bimetallic Pd-Ag/Al_2O_3. *React. Kinet. Catal. Lett.* **2007**, *90*, 107–115. [CrossRef]
43. Yang, L.; Shan, S.; Loukrakpam, R.; Petkov, V.; Ren, Y.; Wanjala, B.N.; Engelhard, M.H.; Luo, J.; Yin, J.; Chen, Y.; et al. Role of support-nanoalloy interactions in the atomic-scale structural and chemical ordering for tuning catalytic sites. *J. Am. Chem. Soc.* **2012**, *134*, 15048–15060. [CrossRef] [PubMed]
44. Shan, S.Y.; Petkov, V.; Yang, L.F.; Mott, D.; Wanjala, B.N.; Cai, F.; Chen, B.H.; Luo, J.; Zhong, C.J. Oxophilicity and Structural Integrity in Maneuvering Surface Oxygenated Species on Nanoalloys in CO Oxidation. *ACS Catal.* **2013**, *3*, 3075–3085. [CrossRef]